Published in final edited form as:
J Cell Physiol. 2012 January ; 227(1): 269–277. doi:10.1002/jcp.22730.

GREMLIN1 IS REQUIRED FOR SKELETAL DEVELOPMENT AND POSTNATAL SKELETAL HOMEOSTASIS

Ernesto Canalis[1,2,*], **Kristen Parker**[1], and **Stefano Zanotti**[1,2]

[1] Department of Research, Saint Francis Hospital and Medical Center, 114 Woodland Street, Hartford, CT, 06105, USA

[2] The University of Connecticut School of Medicine, 263 Farmington Avenue, Farmington, CT, 06030, USA

Abstract

Gremlin is an antagonist of bone morphogenetic proteins, and its overexpression causes suppressed osteoblastogenesis and osteopenia. Inactivation of *Grem1* results in severe developmental defects, but the consequences of the global inactivation of *Grem1* on the postnatal skeleton are not known. To study the function of gremlin, *Grem1* was inactivated by homologous recombination, and mice were maintained in a C57BL/6/FVB mixed genetic background due to embryonic and neonatal lethality in the uniform C57BL/6 background. *Grem1* null mice exhibited developmental skeletal abnormalities, leading to incomplete formation of metatarsal bones and of fore limbs and hind limbs. *Grem1* null mice exhibited decreased weight and body fat and shortened femoral length. Bone histomorphometric and microarchitectural analyses of distal femurs revealed decreased bone volume and increased bone formation in 1 month old *Grem1* null mice. Trabecular femoral bone volume was restored in older *Grem1* null female mice, and to a lesser extent in male mice. Vertebral microarchitecture confirmed the osteopenia observed in 1 month old *Grem1* null mice and demonstrated recovery of trabecular bone in older female, but not in older male *Grem1* null mice, which exhibited persistent vertebral osteopenia. In conclusion, *Grem1* is not only necessary for skeletal development, but also for postnatal skeletal homeostasis; its inactivation causes osteopenia, which is partially reversed in a spatial, temporal and sex-dependent manner due to an increase in bone formation.

Keywords

bone formation; bone morphogenetic protein (BMP); BMP antagonists; noggin; gremlin

INTRODUCTION

Bone morphogenetic proteins (BMPs) play a role in the regulation of osteoblastogenesis and endochondral bone formation (Canalis et al, 2003). BMPs induce the differentiation of mesenchymal cells toward the osteoblastic lineage and enhance the pool and function of mature osteoblasts (Canalis et al, 2003; Ghosh-Choudhury et al, 1994; Thies et al, 1992). Upon ligand binding, BMPs initiate a signal transduction cascade activating the mothers against the decapentaplegic (Smad) or the mitogen-activated protein kinase signaling pathways (Canalis et al, 2003; Miyazono, 1999; Nohe et al, 2002). In osteoblastic cells, BMPs primarily utilize the Smad signaling pathway (Deregowski et al, 2006; Zanotti et al,

[*]Address correspondence and reprint requests to: Ernesto Canalis, M.D., Department of Research, Saint Francis Hospital and Medical Center, 114 Woodland Street, Hartford, CT 06105-1299, Tel: (860)714-4068, Fax: (860)714-8053, ECanalis@stfranciscare.org.

2008). The activity of BMPs is controlled by a large group of secreted polypeptides that prevent BMP signaling by binding BMPs and by precluding ligand-receptor interactions (Canalis et al, 2003; Gazzerro and Canalis, 2006).

Gremlin is a member of the *Differentially screening-selected gene aberrative in neuroblastoma* (*Dan*)/*Cerberus* family of genes and two *Gremlin* genes have been described, namely *Gremlin1* (*Grem1*) and *Gremlin2* or *Protein related to Dan and Cerberus* (Hsu et al, 1998; Sudo et al, 2004; Topol et al, 1997). *Grem1* and its rat ortholog, *Down regulated by v-mos*, encode secreted glycoproteins with a molecular mass of 20.7 kilo Daltons (Topol et al, 2000). Gremlin1 (subsequently termed gremlin) binds and prevents the activity of BMP-2, -4 and -7, and similarly to other BMP antagonists, it inhibits Wnt activity (Canalis et al, 2003; Gazzerro et al, 2005; Winkler et al, 2005). Gremlin is expressed by stromal cells surrounding certain neoplastic cells, and it is considered to play a role in cell survival and possibly tumorigenesis (Sneddon et al, 2006; Topol et al, 2000). The patterning of distal limb skeletal elements is tightly regulated by the reciprocal interactions between BMPs, fibroblast growth factors (FGFs) 4 and 8 and Sonic hedgehog (SHH) (Khokha et al, 2003). By inhibiting BMP action, gremlin allows for FGF 4/8 expression, which in turn promotes SHH expression in the posterior limb bud, and SHH is required for proper limb patterning and development. Homozygous null mutations of *Grem1* in mice result in serious developmental limb, metanephric and lung abnormalities, leading to absent kidneys and intrauterine or newborn lethality (Khokha et al, 2003; Michos et al, 2004).

Later in skeletal development, after the pattern of skeletal elements has been established, *Grem1* is expressed by osteoblasts, where its transcription is induced by BMPs (Pereira et al, 2000). Transgenics overexpressing gremlin under the control of the osteocalcin promoter exhibit decreased bone formation leading to osteopenia and long bone fractures (Gazzerro et al, 2005). Overexpression of gremlin in bone marrow stromal cells decreases BMP/Smad signaling and opposes the effect of BMP-2 on osteoblastogenesis, confirming that gremlin is a BMP antagonist in skeletal tissue (Gazzerro et al, 2005). Inactivation of *Grem1* in a homogeneous C57BL/6 genetic background is lethal (Khokha et al, 2003; Michos et al, 2004); and the conditional inactivation of *Grem1* in mature osteoblasts causes a transient increase in bone volume secondary to an increase in bone formation (Gazzerro et al, 2007). Recently, we observed survival of mice carrying the global deletion of *Grem1* in a mixed C57BL/6/Friend virus B type (FVB) genetic background. These mice would allow a study of the postnatal and adult phenotype caused by the global inactivation of *Grem1*. The intent of the present study was to define the function of gremlin in skeletal tissue *in vivo*. For this purpose, we determined the general characteristics, the body composition and the histomorphometric and skeletal microarchitectural properties of *Grem1* null mice from 10 days through 6 months of age.

MATERIALS AND METHODS

Grem1 Null Mice

Heterozygous $Grem1^{+/LacZ}$ (subsequently termed $Grem1^{+/-}$) null mice in a C57BL/6 genetic background were obtained from R. Harland (Berkley, CA) and were crossed with FVB wild type mice (Khokha et al, 2003). Heterozygous mice carrying the deleted *Grem1* gene were intercrossed to obtain homozygous null mice and wild type littermate controls. *Grem1* null mice were genotyped by polymerase chain reaction (PCR) using 5′-CTTATTGTCTGTGTCCCCCTC-3′ (forward) and 5′-AGGGGACGACGACAGTATCG-3′ (reverse) primers. The *Grem1* null state was confirmed by documenting absence of gremlin mRNA in calvarial extracts by real time reverse transcription (RT)-PCR (Nazarenko et al, 2002a; Nazarenko et al, 2002b). *Grem1* null mice were compared to wild type littermate controls following the intermating of *Grem1* heterozygous mice. All animal experiments

were approved by the Animal Care and Use Committee of Saint Francis Hospital and Medical Center.

X-ray Analysis, Bone Mineral Density (BMD), Body Composition and Femoral Length

X-rays were performed on eviscerated mice at an intensity of 30 kV for 20 seconds on a Faxitron X-ray system (model MX 20, Faxitron X-Ray Corp., Wheeling, IL). Total BMD (g/cm^2) and total body fat (g) were measured on anesthetized mice using the PIXImus small animal DEXA system (GE Medical System/LUNAR, Madison, WI) (Nagy et al, 2001). Femoral images were used to determine femoral length in mm. Calibrations were performed with a phantom of defined value, and quality assurance measurements were performed before each use. The coefficient of variation for total BMD was less than 1% (n = 9).

Bone Histomorphometric Analysis

Static and dynamic histomorphometry were carried out on *Grem1* null and control mice after they were injected with calcein, 20 mg/kg, and demeclocycline, 50 mg/kg, at an interval of 2 days for 1 month old animals and 7 days for 3 and 6 month old animals. Mice were sacrificed by CO_2 inhalation 2 days after the demeclocycline injection. In 10 day old mice only static histomorphometry was performed. Femurs and vertebrae were dissected and fixed in 70% ethanol, dehydrated and embedded undecalcified in methyl methacrylate. Longitudinal femoral sections, 5 μm thick, were cut on a microtome (Microm, Richards-Allan Scientific, Kalamazoo, MI) and stained with 0.1% toluidine blue or von Kossa. Static parameters of bone formation and resorption were measured in a defined area between 360 μm and 2160 μm from the growth plate, encompassing 2.59 mm^2 of area, using an OsteoMeasure morphometry system (Osteometrics, Atlanta, GA) (Gazzerro et al, 2005). For 10 day old mice, the femoral area measured was between 180 μm and 1660 μm from the growth plate, encompassing an area of 1.27 mm^2. For vertebral histomorphometry, 5 μm thick Lumbar 3 (L3) cross sections were obtained and a 2.59 mm^2 area was measured. For dynamic histomorphometry, mineralizing surface per bone surface and mineral apposition rate were measured on unstained sections under ultraviolet light, using a diamidino-2-phenylindole, fluorescein isothiocyanate, Texas red filter, and bone formation rate was calculated. The terminology and units used are those recommended by the Histomorphometry Nomenclature Committee of the American Society for Bone and Mineral Research (Parfitt et al, 1987).

Microcomputed Tomography (μCT)

Bone microarchitecture of vertebrae and femurs from *Grem1* null and control mice was determined using a Microcomputed Tomographic Instrument (μCT 40; Scanco Medical AG, Bassersdorf, Switzerland) calibrated weekly using a phantom provided by the manufacturer. The vertebral body of L3 and femurs were scanned in 70% ethanol at high resolution, energy level of 55 kVp, intensity of 145 μA and integration time of 200 ms. Trabecular bone volume fraction and microarchitecture were evaluated starting approximately 1.0 mm from the cranial side of the vertebral body, or 1.0 mm proximal from the femoral condyles. For L3 and femurs, a total of 100 and 160 consecutive slices, respectively, were acquired at an isotropic voxel size of 6 $μm^3$ and a slice thickness of 6 μm, and chosen for analysis. Contours were manually drawn every 10 slices a few voxels away from the endocortical boundary to define the region of interest for analysis. The remaining slice contours were iterated automatically. Trabecular regions were assessed for total volume, bone volume, bone volume fraction (bone volume/total volume), trabecular thickness, trabecular number, trabecular separation, connectivity density and structural model index using a Gaussian filter ($\sigma = 0.8$, support = 1) and user defined threshold (Bouxsein et al, 2010; Glatt et al, 2007). For analysis of femoral cortical bone, contours were iterated across 100 slices along the

cortical shell, excluding the marrow cavity. Analysis of cortical thickness was performed using a Gaussian filter (σ = 0.8, support = 1) and user defined threshold.

Real Time RT-PCR

Total RNA was extracted from calvariae and mRNA levels determined by real time RT-PCR (Nazarenko et al, 2002a; Nazarenko et al, 2002b). RNA was reverse-transcribed using SuperScript III Platinum Two-Step qRT-PCR kit (Invitrogen), according to manufacturer's instructions, and amplified in the presence of 5′-CGGTTAGCCGCACTATCATCAAC[FAM]G-3′ and 5′-GTGAACTTCTTGGGCTTGCAGA-3′ primers for *Grem1*; and 5′-CGAACCGGATAATGTGAAGTTCAAGGTT[FAM]G-3′ and 5′-CTGCTTCAGCTTCTCTGCCTTT-3′ primers for *ribosomal protein L38 (RPL38)*, and Platinum Quantitative PCR SuperMix-UDG (Invitrogen) at 60 °C for 45 cycles. Transcript copy number was estimated by comparison with a standard curve constructed using *Grem1* (Regeneron Pharmaceuticals, Tarrytown, NY) and *Rpl38* (American Type Culture Collection, Manassas, VA) cDNAs. Reactions were conducted in a 96-well spectrofluorometric thermal iCycler (Bio-Rad), and fluorescence was monitored during every PCR cycle at the annealing step. Data are expressed as copy number corrected for *Rpl38*.

Statistical analysis

Data are expressed as means ± SEM. Statistical differences were determined by unpaired Student's *t* test or ANOVA.

RESULTS

General Characteristics of Grem1 Null Mice

To study *Grem1* null mice, $Grem1^{+/-}$ mice, in a C57BL/6/FVB genetic background, were intermated to obtain $Grem1^{-/-}$ mice and wild type littermate controls. The *Grem1* null genotype was documented by PCR of tail extracts, and the *Grem1* null state was confirmed by determining gremlin mRNA levels in calvarial extracts. Gremlin transcripts were detectable in calvariae from wild type controls, but were undetectable in calvariae from *Grem1* null mice from 1 to 6 months of age (Figure 1). *Grem1* heterozygous intermatings yielded the expected Mendelian ratio of 27% $Grem1^{-/-}$, 48% $Grem1^{+/-}$ and 25% wild type mice at birth (n = 241). However, homozygous *Grem1* null mice suffered 51% lethality in the first 24 h after birth. Visual examination of 10 day to 1 month old surviving *Grem1* homozygous null mice revealed that 65% had a single kidney, whereas 35% had two kidneys although in one-third of them one of the kidneys appeared visually small (n = 25). Histological examination of kidneys from 10 day and 1 month old *Grem1* null mice did not reveal any obvious abnormalities, except for occasionally dilated tubules and occasional decreased tubular cellularity (Histoserv, Inc, Germantown, MD). Lung histopathology revealed no abnormalities.

Grem1 null mice were small, and their weight and femoral length were decreased when compared to wild type controls (Figure 1). Percent body fat was not affected at 1 month of age, but it was decreased by 30 to 50% at 3 and 6 months of age (Figure 1). *Grem1* null mice had short fore limbs and hind limbs and incompletely developed feet; and confirming prior observations, contact radiography revealed absent fibula and metatarsal bones in *Grem1* null mice (Figure 2) (Khokha et al, 2003; Michos et al, 2004). Femoral bone mineral density (BMD) was decreased in 1 month old *Grem1* null mice, but not in older mice. At 1 month of age, femoral BMD (means ± SEM; n= 4 to 14) of male control mice was 377 ± 10

and of *Grem1* null mice was 306 ± 14 g/cm^2 × 10^4 (p<0.05); femoral BMD of control female mice was 402 ± 13 and of *Grem1* null mice was 302 ± 11 g/cm^2 × 10^4 (p<0.05).

Femoral Histomorphometry of Grem1 Null Mice

Static bone histomorphometric analysis of femurs from *Grem1* null mice at 10 days of age revealed that they were not different from control mice. However, the amount of trabecular bone present in 10 day old wild type and experimental mice is minimal when compared to older mice, creating potential difficulties in the assessment of a phenotype (Table 1, Figure 3). At 1 month of age, male and female *Grem1* null mice had decreased bone volume/tissue volume secondary to a decrease in trabecular number (Table 1, Figure 3). There was no change in osteoblast number/perimeter or osteoclast number/perimeter, but mineralizing surface was increased causing a 55% increase in bone formation, which was statistically significant in male mice. There were no changes in eroded surface indicating normal bone resorption.

Femoral histomorphometry of male *Grem1* null mice at 3 and 6 months of age revealed a recovery of the osteopenic phenotype, and trabecular bone volume was not significantly different from wild type controls. At 3 months of age, a modest increase in osteoblast number was noted; at 6 months of age a 35%, not statistically significant, decrease in bone volume due to a significant decrease in trabecular number was noted in male *Grem1* null mice (Table 1). Femoral histomorphometry of female *Grem1* null mice revealed an increase in trabecular bone volume/tissue volume at 3 months of age due to an increase in trabecular thickness, followed by a normalization of the trabecular bone volume at 6 months of age (Table 1; Figure 3). There was a tendency toward higher bone formation rates in femurs from 3 month old *Grem1* null male mice and a significant 2.5 fold increase in *Grem1* null female mice possibly explaining the increased trabecular thickness and the recovery of bone volume at 3 and 6 months of age. The increase in bone formation was secondary to increased mineralizing surface, and mineral apposition rate was not different between *Grem1* null mice and controls (Table 1, Figure 3).

Femoral Microarchitecture of Grem1 Null Mice

In accordance with the bone histomorphometric findings, trabecular femoral microarchitecture assessed by μCT revealed that male and female *Grem1* null mice were osteopenic at 1 month of age due to a decreased number of trabeculae (Table 2). The osteopenia was associated with decreased connectivity and a tendency toward rod-like trabeculae. Cortical thickness was decreased in 1 month old *Grem1* null mice. In male *Grem1* null mice, the trabecular microarchitectural changes appeared to be more evident and persistent than in female mice. Although they were not observed at 3 months of age, they recurred at 6 months of age when *Grem1* null male mice exhibited osteopenia. In contrast, the loss of trabecular and cortical bone observed in 1 month old *Grem1* female null mice was transient and not present at 3 and 6 months of age. This is in accordance with the recovery of trabecular bone volume observed by histomorphometry.

Vertebral Microarchitecture and Histomorphometry of Grem1 Null Mice

Skeletal microarchitecture was examined in L3 vertebrae from *Grem1* null and control mice. Analysis of L3 was performed to assess whether the osteopenic phenotype observed in *Grem1* null mice was secondary to the limb abnormalities described. Confirming the femoral histomorphometric analysis, both male and female *Grem1* null mice exhibited vertebral osteopenia at 1 month of age (Table 3, Figure 4). In accordance with the femoral phenotype, the vertebral osteopenia was transient in female *Grem1* null mice. In contrast, the vertebral osteopenia was sustained in male mice, which exhibited decreased trabecular number and connectivity from 1 to 6 months of age. Trabecular structure was more rod-like

in *Grem1* null male mice than in wild type controls, confirming changes in bone microarchitecture.

Histomorphometric analysis of L3 vertebrae from 3 month old *Grem1* null mice confirmed the osteopenic phenotype in male mice despite an increase in osteoblast number and bone formation rate (Table 4). In accordance with the μCT findings, 3 month old *Grem1* null female mice were not osteopenic. An insufficient number of 3 month old female mice had calcein and demeclocycline dual labels so that dynamic vertebral histomorphometry could not be analyzed in female mice.

DISCUSSION

Our findings confirm that *Grem1* null mice exhibit abnormal limb and renal development. We demonstrate that when in a mixed genetic composition (C57BL/6/FVB) ~50% of *Grem1* null mice survive, although they are small and have decreased femoral length possibly due to limb developmental abnormalities. Gremlin is expressed by the metanephric mesenchyme, is essential for metanephric kidney development and its antagonism of BMPs promote survival of mesenchymal cells (Khokha et al, 2003; Michos et al, 2004). In the absence of gremlin, mesenchymal cell death occurs, explaining the absence of one kidney in 65% of surviving *Grem1* null mice.

Grem1 null male and female mice exhibited impaired growth and femoral osteopenia at 1 month of age. It is possible that the femoral osteopenia was in part related to an incomplete limb development. However, additional factors seemed to have played a role in their skeletal phenotype since 10 day old *Grem1* null mice were not osteopenic, and the osteopenia was also present in L3 vertebrae. This would suggest a generalized impact of the *Grem1* inactivation on the skeleton. It is of interest that the osteopenia observed was of a transient nature, particularly in female *Grem1* null mice, which exhibited recovery of trabecular bone both at femoral and vertebral sites at 3 and 6 months of age. A temporally and spatially dependent limited recovery was observed in male *Grem1* null mice since the bone volume transiently normalized in the femur, but not at vertebral sites. The reason for the greater recovery of trabecular bone at femoral sites and in female *Grem1* null mice is not immediately apparent. At femoral sites, the sexual dimorphism might be attributed to a more rapid age-dependent decline in trabecular bone volume in wild type female than in male mice, but this does not explain the sexual dimorphism observed at vertebral sites (Glatt et al, 2007). The reversal of the osteopenic phenotype can be explained by an increase in bone formation in *Grem1* null mice. In female mice, this increase may have been sufficient to prevent the normal decline of femoral trabecular bone observed in wild type controls and even to cause a transient increase in femoral trabecular bone volume at 3 months of age. The increase in bone formation was not sufficient to normalize vertebral trabecular bone volume in male mice, suggesting that gremlin impacts other aspects of skeletal homeostasis.

The enhanced bone formation in *Grem1* null mice was secondary to an increase in mineralizing surface and not in mineral apposition rate. This indicates an increase in areas actively forming bone and not in the function of individual osteoblasts, and may be related to the increase in osteoblast number observed in 3 month old male mice. Changes in mineralizing surface responsible for changes in bone formation are not unusual, and were found in *Cebp homologous protein* null mice and in female *Sost* null mice (Pereira et al, 2006; Li et al, 2008). They were also reported in *Cynomolgus* monkeys treated with sclerostin antibodies, which exhibited a pronounced enhancement in mineralizing surface and a modest change in mineral apposition rate (Ominsky et al, 2010). The increased bone formation observed in *Grem1* null mice confirms results observed following the conditional deletion of *Grem1* in osteoblasts, and is in agreement with the suppression of bone

formation observed in transgenic mice overexpressing gremlin in osteoblasts (Gazzerro et al, 2005; Gazzerro et al, 2007). It is also in accordance with previous studies from this laboratory demonstrating that down regulation of *Grem1* by RNA interference sensitizes osteoblastic cells to the actions of BMP-2 (Gazzerro et al, 2007). Stabilization of femoral trabecular bone volume instead of an increase in bone volume in older male and female *Grem1* null mice may have been the result of a limited amount of trabecular bone present in femurs, and the preponderance of cortical bone. However, it is also possible that the activity of BMP-2 is not sufficiently or permanently enhanced in the context of the *Grem1* inactivation to cause a more permanent phenotype or that BMP-2 does not have an effect on skeletal homeostasis of older mice.

The phenotype of the *Grem1* global inactivation resembles that observed following the inactivation of *Connective tissue growth factor* (*Ctgf*), a member of the Cyr61, CTGF, Nov, (CCN) family of proteins known to bind and antagonize BMP action (Abreu et al, 2002; Brigstock, 2003; Canalis et al, 2010). It is of interest that, like in the case of gremlin, transgenic overexpression of CTGF causes osteopenia, whereas its inactivation reveals that it is necessary for skeletal homeostasis (Canalis et al, 2010; Smerdel-Ramoya et al, 2008). These observations suggest that when in excess BMP antagonists inhibit BMP actions and bone formation, but basal levels of BMP antagonists are required to maintain bone homeostasis, possibly by tempering selected BMP actions.

The *in vivo* phenotype described indicates that gremlin is not only required for normal skeletal development, but also for normal postnatal bone remodeling since *Grem1* inactivation leads to osteopenia in adult male mice, particularly at vertebral sites. It is possible that the osteopenia observed in *Grem1* null mice represents sensitization of BMP signaling and an increase in bone resorption caused by BMP-2 (Mandal et al, 2009; Okamoto et al, 2006; Sotillo Rodriguez et al, 2009). However, if the phenotype observed was secondary to increased bone resorption, this would have been modest and transient because bone histomorphometry did not reveal changes in osteoclast number or eroded surface. It is possible that enhanced BMP activity due to decreased levels of gremlin results in increased expression of the Wnt antagonists dickkopf and sclerostin and suppressed Wnt signaling, which may explain the transient osteopenic phenotype observed (Kamiya et al, 2008; Kamiya et al, 2010). However, gremlin, like other BMP antagonists, suppresses Wnt signaling and one would expect sensitization of Wnt signaling in the absence of gremlin (Gazzerro et al, 2005; Gazzerro et al, 2007; Westendorf et al, 2004). Another possible explanation of the osteopenic phenotype is the induction of noggin expression, another BMP antagonist, following enhanced BMP signaling in the absence of gremlin since noggin in excess causes osteopenia (Devlin et al, 2003; Gazzerro et al, 1998). Although most of the activities of gremlin are explained by its capacity to bind and block BMP activity, effects independent of BMP interactions have not been completely excluded (Canalis et al, 2003). For example, gremlin is expressed by tumor cells and may favor tumor cell survival (Sneddon et al, 2006). Consequently, the osteopenic phenotype observed following the inactivation of *Grem1* may be explained by direct effects of gremlin in skeletal cell function.

The results observed in *Grem1* null mice differ from those reported following the global inactivation of genes encoding the Wnt antagonists, sclerostin and dickkopf 1 (Li et al, 2008; Morvan et al, 2006). The deletion of *Sost*, encoding for sclerostin, or the haploinsufficiency of *Dickkopf1* cause increased bone formation and bone mass, indicating that these antagonists could be targeted to enhance Wnt activity as possible therapeutic approaches in the management of osteoporosis. The results we describe in *Grem1* null mice suggest that neutralization of gremlin to enhance BMP activity may cause osteopenia, and not yield a sustained increase in bone formation and bone mass. Consequently, data derived from the mouse models described suggest that the suppression of Wnt antagonists may result

in a skeletal anabolic effect, whereas the suppression of gremlin may not. Recent investigations have demonstrated that the administration of either anti-sclerostin or anti-dickkopf 1 antibodies increase bone formation and bone mass in experimental murine and non-human primate models (Glantschnig et al, 2010; Li et al, 2009; Ominsky et al, 2010).

In conclusion, our studies reveal that gremlin is required for skeletal development and adult skeletal homeostasis; *Grem1* inactivation causes osteopenia, and increased bone formation that reverses the osteopenia, preferentially at femoral sites and in female mice.

Acknowledgments

The authors thank Regeneron Pharmaceuticals for gremlin cDNA, R. Harland for *Grem1* null mice, Allison Kent for technical assistance and Mary Yurczak for secretarial assistance.

This work was supported by Grant AR021707 (EC) from the National Institute of Arthritis and Musculoskeletal and Skin Diseases.

ABBREVIATIONS

BMD	bone mineral density
BMP	bone morphogenetic protein
CCN	Cyr61, CTGF, Nov
CTGF	connective tissue growth factor
Dan	Differentially screening-selected gene aberrative in neuroblastoma
FGF	fibroblast growth factor
FVB	Friend virus B type
Grem1	Gremlin1
μCT	microcomputed tomography
PCR	polymerase chain reaction
RPL38	ribosomal protein L38
RT-PCR	reverse transcription PCR
Smad	Signaling mothers against decapentaplegic
SHH	Sonic hedgehog

References

Abreu JG, Ketpura NI, Reversade B, De Robertis EM. Connective-tissue growth factor (CTGF) modulates cell signalling by BMP and TGF-beta. Nat Cell Biol. 2002; 4:599–604. [PubMed: 12134160]

Bouxsein ML, Boyd SK, Christiansen BA, Guldberg RE, Jepsen KJ, Muller R. Guidelines for assessment of bone microstructure in rodents using micro-computed tomography. J Bone Miner Res. 2010; 25:1468–1486. [PubMed: 20533309]

Brigstock DR. The CCN family: a new stimulus package. J Endocrinol. 2003; 178:169–175. [PubMed: 12904165]

Canalis E, Economides AN, Gazzerro E. Bone morphogenetic proteins, their antagonists, and the skeleton. Endocr Rev. 2003; 24:218–235. [PubMed: 12700180]

Canalis E, Zanotti S, Beamer WG, Economides AN, Smerdel-Ramoya A. Connective Tissue Growth Factor Is Required for Skeletal Development and Postnatal Skeletal Homeostasis in Male Mice. Endocrinology. 2010; 151:3490–3501. [PubMed: 20534727]

Deregowski V, Gazzerro E, Priest L, Rydziel S, Canalis E. Notch 1 Overexpression Inhibits Osteoblastogenesis by Suppressing Wnt/beta-Catenin but Not Bone Morphogenetic Protein Signaling. J Biol Chem. 2006; 281:6203–6210. [PubMed: 16407293]

Devlin RD, Du Z, Pereira RC, Kimble RB, Economides AN, Jorgetti V, Canalis E. Skeletal overexpression of noggin results in osteopenia and reduced bone formation. Endocrinology. 2003; 144:1972–1978. [PubMed: 12697704]

Gazzerro E, Canalis E. Bone morphogenetic proteins and their antagonists. Rev Endocr Metab Disord. 2006; 7:51–65. [PubMed: 17029022]

Gazzerro E, Gangji V, Canalis E. Bone morphogenetic proteins induce the expression of noggin, which limits their activity in cultured rat osteoblasts. J Clin Invest. 1998; 102:2106–2114. [PubMed: 9854046]

Gazzerro E, Pereira RC, Jorgetti V, Olson S, Economides AN, Canalis E. Skeletal overexpression of gremlin impairs bone formation and causes osteopenia. Endocrinology. 2005; 146:655–665. [PubMed: 15539560]

Gazzerro E, Smerdel-Ramoya A, Zanotti S, Stadmeyer L, Durant D, Economides AN, Canalis E. Conditional deletion of gremlin causes a transient increase in bone formation and bone mass. J Biol Chem. 2007; 282:31549–31557. [PubMed: 17785465]

Ghosh-Choudhury N, Harris MA, Feng JQ, Mundy GR, Harris SE. Expression of the BMP 2 gene during bone cell differentiation. Crit Rev Eukaryot Gene Expr. 1994; 4:345–355. [PubMed: 7881166]

Glantschnig H, Hampton RA, Lu P, Zhao JZ, Vitelli S, Huang L, Haytko P, Cusick T, Ireland C, Jarantow SW, Ernst R, Wei N, Nantermet P, Scott KR, Fisher JE, Talamo F, Orsatti L, Reszka AA, Sandhu P, Kimmel D, Flores O, Strohl W, An Z, Wang F. Generation and selection of novel fully human monoclonal antibodies that neutralize Dickkopf-1 (DKK1) inhibitory function in vitro and increase bone mass in vivo. J Biol Chem. 2010; 285:40135–40147. [PubMed: 20929859]

Glatt V, Canalis E, Stadmeyer L, Bouxsein ML. Age-Related Changes in Trabecular Architecture Differ in Female and Male C57BL/6J Mice. J Bone Miner Res. 2007; 22:1197–1207. [PubMed: 17488199]

Hsu DR, Economides AN, Wang X, Eimon PM, Harland RM. The Xenopus dorsalizing factor Gremlin identifies a novel family of secreted proteins that antagonize BMP activities. Mol Cell. 1998; 1:673–683. [PubMed: 9660951]

Kamiya N, Kobayashi T, Mochida Y, Yu PB, Yamauchi M, Kronenberg HM, Mishina Y. Wnt inhibitors Dkk1 and Sost are downstream targets of BMP signaling through the type IA receptor (BMPRIA) in osteoblasts. J Bone Miner Res. 2010; 25:200–210. [PubMed: 19874086]

Kamiya N, Ye L, Kobayashi T, Mochida Y, Yamauchi M, Kronenberg HM, Feng JQ, Mishina Y. BMP signaling negatively regulates bone mass through sclerostin by inhibiting the canonical Wnt pathway. Development. 2008; 135:3801–3811. [PubMed: 18927151]

Khokha MK, Hsu D, Brunet LJ, Dionne MS, Harland RM. Gremlin is the BMP antagonist required for maintenance of Shh and Fgf signals during limb patterning. Nat Genet. 2003; 34:303–307. [PubMed: 12808456]

Li X, Ominsky MS, Niu QT, Sun N, Daugherty B, D'Agostin D, Kurahara C, Gao Y, Cao J, Gong J, Asuncion F, Barrero M, Warmington K, Dwyer D, Stolina M, Morony S, Sarosi I, Kostenuik PJ, Lacey DL, Simonet WS, Ke HZ, Paszty C. Targeted deletion of the sclerostin gene in mice results in increased bone formation and bone strength. J Bone Miner Res. 2008; 23:860–869. [PubMed: 18269310]

Li X, Ominsky MS, Warmington KS, Morony S, Gong J, Cao J, Gao Y, Shalhoub V, Tipton B, Haldankar R, Chen Q, Winters A, Boone T, Geng Z, Niu QT, Ke HZ, Kostenuik PJ, Simonet WS, Lacey DL, Paszty C. Sclerostin antibody treatment increases bone formation, bone mass, and bone strength in a rat model of postmenopausal osteoporosis. J Bone Miner Res. 2009; 24:578–588. [PubMed: 19049336]

Mandal CC, Ghosh CG, Ghosh-Choudhury N. Phosphatidylinositol 3 kinase/Akt signal relay cooperates with smad in bone morphogenetic protein-2-induced colony stimulating factor-1 (CSF-1) expression and osteoclast differentiation. Endocrinology. 2009; 150:4989–4998. [PubMed: 19819979]

Michos O, Panman L, Vintersten K, Beier K, Zeller R, Zuniga A. Gremlin-mediated BMP antagonism induces the epithelial-mesenchymal feedback signaling controlling metanephric kidney and limb organogenesis. Development. 2004; 131:3401–3410. [PubMed: 15201225]

Miyazono K. Signal transduction by bone morphogenetic protein receptors: functional roles of Smad proteins. Bone. 1999; 25:91–93. [PubMed: 10423029]

Morvan F, Boulukos K, Clement-Lacroix P, Roman RS, Suc-Royer I, Vayssiere B, Ammann P, Martin P, Pinho S, Pognonec P, Mollat P, Niehrs C, Baron R, Rawadi G. Deletion of a single allele of the Dkk1 gene leads to an increase in bone formation and bone mass. J Bone Miner Res. 2006; 21:934–945. [PubMed: 16753024]

Nagy TR, Prince CW, Li J. Validation of peripheral dual-energy X-ray absorptiometry for the measurement of bone mineral in intact and excised long bones of rats. J Bone Miner Res. 2001; 16:1682–1687. [PubMed: 11547838]

Nazarenko I, Lowe B, Darfler M, Ikonomi P, Schuster D, Rashtchian A. Multiplex quantitative PCR using self-quenched primers labeled with a single fluorophore. Nucleic Acids Res. 2002a; 30:e37. [PubMed: 11972352]

Nazarenko I, Pires R, Lowe B, Obaidy M, Rashtchian A. Effect of primary and secondary structure of oligodeoxyribonucleotides on the fluorescent properties of conjugated dyes. Nucleic Acids Res. 2002b; 30:2089–2195. [PubMed: 11972350]

Nohe A, Hassel S, Ehrlich M, Neubauer F, Sebald W, Henis YI, Knaus P. The mode of bone morphogenetic protein (BMP) receptor oligomerization determines different BMP-2 signaling pathways. J Biol Chem. 2002; 277:5330–5338. [PubMed: 11714695]

Okamoto M, Murai J, Yoshikawa H, Tsumaki N. Bone morphogenetic proteins in bone stimulate osteoclasts and osteoblasts during bone development. J Bone Miner Res. 2006; 21:1022–1033. [PubMed: 16813523]

Ominsky MS, Vlasseros F, Jolette J, Smith SY, Stouch B, Doellgast G, Gong J, Gao Y, Cao J, Graham K, Tipton B, Cai J, Deshpande R, Zhou L, Hale MD, Lightwood DJ, Henry AJ, Popplewell AG, Moore AR, Robinson MK, Lacey DL, Simonet WS, Paszty C. Two doses of sclerostin antibody in cynomolgus monkeys increases bone formation, bone mineral density, and bone strength. J Bone Miner Res. 2010; 25:948–959. [PubMed: 20200929]

Parfitt AM, Drezner MK, Glorieux FH, Kanis JA, Malluche H, Meunier PJ, Ott SM, Recker RR. Bone histomorphometry: standardization of nomenclature, symbols, and units. Report of the ASBMR Histomorphometry Nomenclature Committee. J Bone Miner Res. 1987; 2:595–610. [PubMed: 3455637]

Pereira RC, Economides AN, Canalis E. Bone morphogenetic proteins induce gremlin, a protein that limits their activity in osteoblasts. Endocrinology. 2000; 141:4558–4563. [PubMed: 11108268]

Pereira RC, Stadmeyer L, Marciniak SJ, Ron D, Canalis E. C/EBP homologous protein is necessary for normal osteoblastic function. J Cell Biochem. 2006; 97:633–640. [PubMed: 16220546]

Smerdel-Ramoya A, Zanotti S, Stadmeyer L, Durant D, Canalis E. Skeletal Overexpression Of Connective Tissue Growth Factor (CTGF) Impairs Bone Formation And Causes Osteopenia. Endocrinology. 2008; 149:4374–4381. [PubMed: 18535099]

Sneddon JB, Zhen HH, Montgomery K, van de RM, Tward AD, West R, Gladstone H, Chang HY, Morganroth GS, Oro AE, Brown PO. Bone morphogenetic protein antagonist gremlin 1 is widely expressed by cancer-associated stromal cells and can promote tumor cell proliferation. Proc Natl Acad Sci U S A. 2006; 103:14842–14847. [PubMed: 17003113]

Sotillo Rodriguez JE, Mansky KC, Jensen ED, Carlson AE, Schwarz T, Pham L, Mackenzie B, Prasad H, Rohrer MD, Petryk A, Gopalakrishnan R. Enhanced osteoclastogenesis causes osteopenia in twisted gastrulation-deficient mice through increased BMP signaling. J Bone Miner Res. 2009; 24:1917–1926. [PubMed: 19419314]

Sudo S, vsian-Kretchmer O, Wang LS, Hsueh AJ. Protein related to DAN and cerberus is a bone morphogenetic protein antagonist that participates in ovarian paracrine regulation. J Biol Chem. 2004; 279:23134–23141. [PubMed: 15039429]

Thies RS, Bauduy M, Ashton BA, Kurtzberg L, Wozney JM, Rosen V. Recombinant human bone morphogenetic protein-2 induces osteoblastic differentiation in W-20-17 stromal cells. Endocrinology. 1992; 130:1318–1324. [PubMed: 1311236]

Topol LZ, Bardot B, Zhang Q, Resau J, Huillard E, Marx M, Calothy G, Blair DG. Biosynthesis, post-translation modification, and functional characterization of Drm/Gremlin. J Biol Chem. 2000; 275:8785–8793. [PubMed: 10722723]

Topol LZ, Marx M, Laugier D, Bogdanova NN, Boubnov NV, Clausen PA, Calothy G, Blair DG. Identification of drm, a novel gene whose expression is suppressed in transformed cells and which can inhibit growth of normal but not transformed cells in culture. Mol Cell Biol. 1997; 17:4801–4810. [PubMed: 9234736]

Westendorf JJ, Kahler RA, Schroeder TM. Wnt signaling in osteoblasts and bone diseases. Gene. 2004; 341:19–39. [PubMed: 15474285]

Winkler DG, Sutherland MS, Ojala E, Turcott E, Geoghegan JC, Shpektor D, Skonier JE, Yu C, Latham JA. Sclerostin inhibition of Wnt-3a-induced C3H10T1/2 cell differentiation is indirect and mediated by bone morphogenetic proteins. J Biol Chem. 2005; 280:2498–2502. [PubMed: 15545262]

Zanotti S, Smerdel-Ramoya A, Stadmeyer L, Canalis E. Activation of the ERK pathway in osteoblastic cells, role of gremlin and BMP-2. J Cell Biochem. 2008; 104:1421–1426. [PubMed: 18286547]

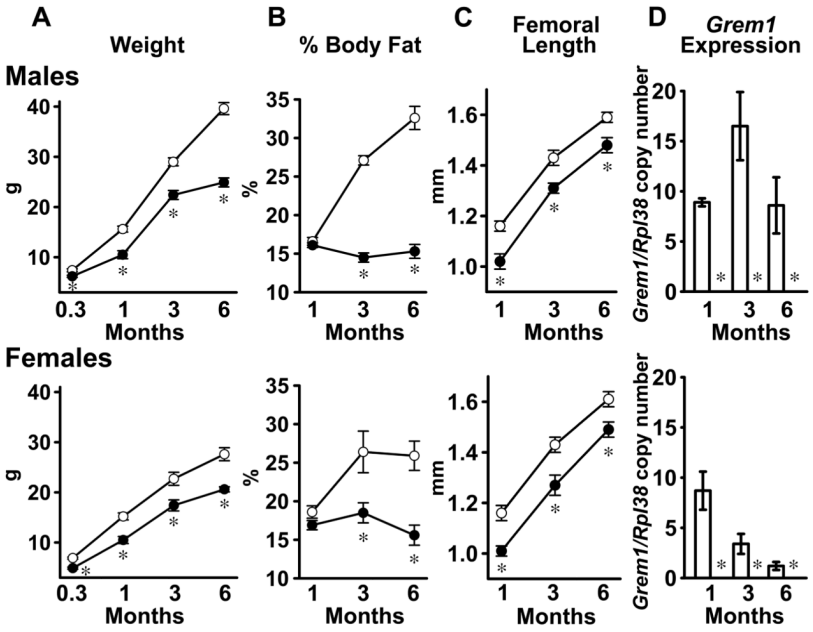

Figure 1.

Weight, body composition (% fat), femoral length and real time RT-PCR of calvarial RNA extracts from 1, 3 and 6 month old male (upper panels) and female (lower panels) *Grem1* null mice (filled circles and black bars) and wild type littermate controls (open circles and white bars). The weight in g, also obtained in 10 day old mice, (A); % body fat (B); femoral length in mm (C); and *Grem1* copy number corrected for *Rpl38* (D) are shown. Please note *Grem1* was undetectable in *Grem1* null mice so that bars are not depicted. Values are means ± SEM, n = 4 to 14. *Significantly different from control mice, $p < 0.05$.

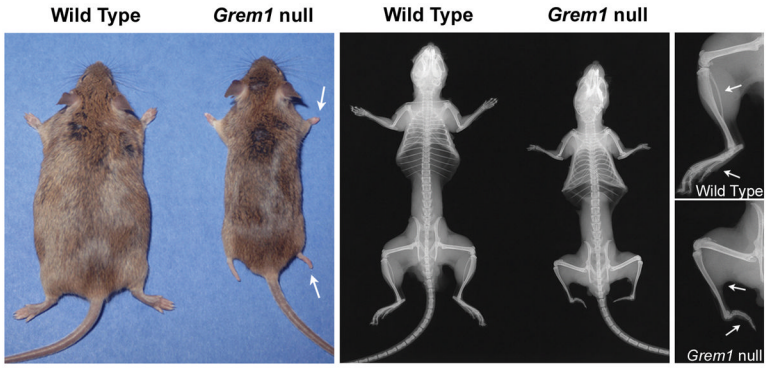

Figure 2.
Representative photographs and skeletal X-rays of 3 month old *Grem1* null mice and wild type (WT) littermate controls. Arrows point to absent fibula and metatarsal bones.

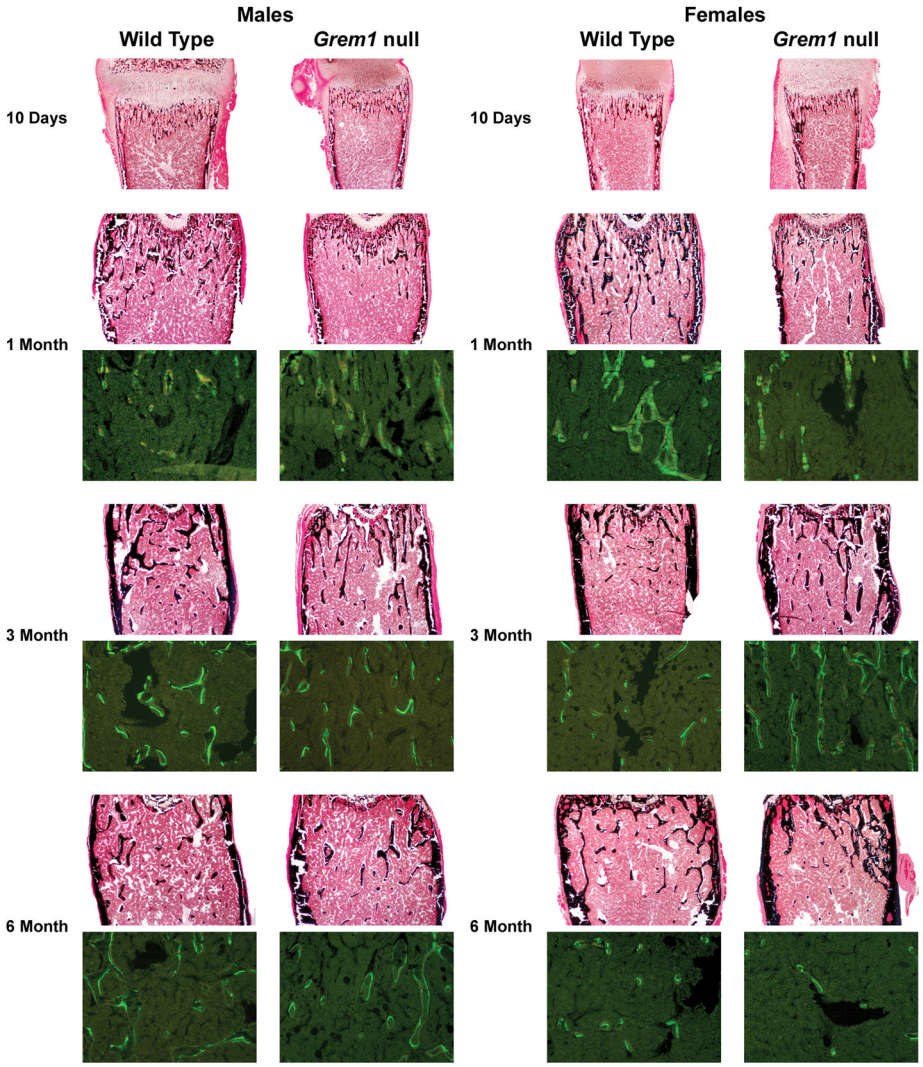

Figure 3.

Representative histological sections and calcein/demeclocycline labeling of femoral sections from 10 day and 1, 3 and 6 month old male and female *Grem1* null mice and wild type littermate controls. Sections were stained with von Kossa without counter stain (final magnification 40×) at all ages or unstained and examined under fluorescence microscopy at 1, 3 and 6 months of age (final magnification 100×).

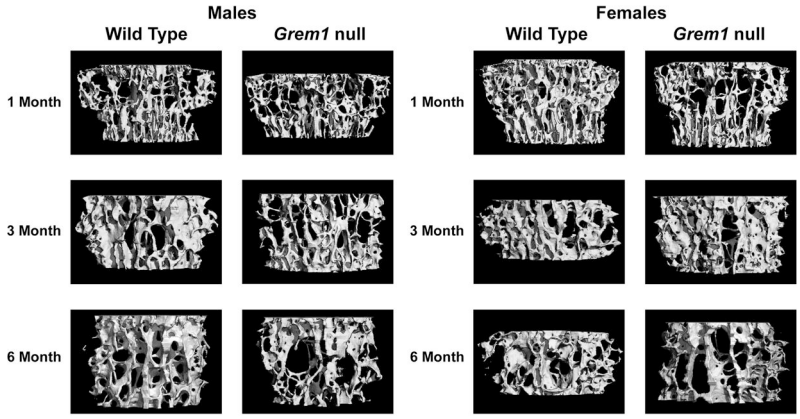

Figure 4.
Representative vertebral microarchitecture assessed by μCT scanning of 1, 3 and 6 month old male and female *Grem1* null mice and wild type littermate controls.

Table 1

Femoral histomorphometry of 10 day, 1, 3 and 6 month old male and female *Grem1* null mice and wild type littermate controls.

Males	**10 Day**		**1 Month**		**3 Month**		**6 Month**	
	Wild Type	***Grem1* null**	**Wild Type**	***Grem1* null**	**Wild Type**	***Grem1* null**	**Wild Type**	***Grem1* null**
Bone Volume/Tissue Volume (%)	3.0 ± 0.3	3.5 ± 1.5	9.5 ± 0.7	6.1 ± 1.2*	11.7 ± 1.4	12.7 ± 3.1	7.1 ± 0.8	4.7 ± 1.1
Trabecular Separation (μm)	452 ± 49	613 ± 120	226 ± 18	375 ± 65*	142 ± 35	135 ± 34	345 ± 31	599 ± 126*
Trabecular Number (1/mm)	2.3 ± 0.2	2.4 ± 0.9	4.3 ± 0.3	2.9 ± 0.5*	8.2 ± 1.2	8.0 ± 1.5	2.8 ± 0.2	1.9 ± 0.3*
Trabecular Thickness (μm)	13.1 ± 0.6	13.4 ± 1.5	22.3 ± 0.7	20.6 ± 1.8	16.5 ± 2.7	16.1 ± 2.0	24.7 ± 1.3	23.3 ± 2.2
Osteoblast Surface/Bone Surface (%)	13.9 ± 1.4	12.1 ± 2.3	16.7 ± 1.5	17.2 ± 3.2	10.3 ± 1.6	16.3 ± 2.9	9.4 ± 0.9	10.6 ± 1.7
Number of Osteoblasts/Bone Perimeter (1/mm)	14.8 ± 1.7	12.8 ± 2.6	15.5 ± 1.5	16.1 ± 3.0	19.5 ± 1.7	31.1 ± 4.9*	11.2 ± 0.9	13.4 ± 1.8
Number of Osteoblasts/Tissue Area (1/mm^2)	70 ± 11	60 ± 22	101 ± 11	77 ± 22	259 ± 46	391 ± 95	49 ± 5	40 ± 9
Osteoclast Surface/Bone Surface (%)	14.2 ± 1.2	15.5± 0.9	14.4 ± 0.9	13.8 ± 0.5	10.5 ± 0.4	10.7 ± 1.0	11.4 ± 1.2	11.3 ± 1.1
Number of Osteoclasts/Bone Perimeter (1/mm)	9.9 ± 0.9	10.5 ± 0.7	7.1 ± 0.4	6.5 ± 0.2	8.5 ± 0.7	9.3 ± 1.4	5.4 ± 0.6	5.5 ± 0.6
Number of Osteoclasts/Tissue Area (1/mm^2)	45 ± 5	50 ± 20	46 ± 3	29 ± 5*	113 ± 19	130 ± 37	23 ± 3	16 ± 3
Eroded Surface/Bone Surface (%)	28.4 ± 2.1	29.5 ± 1.3	28.3 ± 1.3	25.8 ± 1.0	17.1 ± 0.7	18.2 ± 1.8	17.1 ± 1.8	17.6 ± 1.8
Mineral Apposition Rate (μm/day)			1.86 ± 0.06	1.87 ± 0.16	0.37 ± 0.03	0.40 ± 0.05	0.52 ± 0.02	0.46 ± 0.03
Mineralizing Surface/Bone Surface (%)			4.5 ± 0.5	6.8 ± 1.1*	12.7 ± 2.0	16.5 ± 2.2	9.2 ± 0.9	9.8 ± 1.7
Bone Formation Rate (μm^3/μm^2/day)			0.083 ± 0.010	0.130 ± 0.023*	0.046 ± 0.007	0.064 ± 0.005	0.048 ± 0.005	0.046 ± 0.010
Females	10 Day		1 Month		3 Month		6 Month	
	Wild Type	*Grem1* null	Wild Type	*Grem1* null	Wild Type	*Grem1* null	Wild Type	*Grem1* null
Bone Volume/Tissue Volume (%)	2.1 ± 0.2	1.8 ± 0.3	9.8 ± 0.9	4.2 ± 0.7*	6.1 ± 0.5	10.7 ± 2.1*	5.0 ± 0.5	4.8 ± 1.1
Trabecular Separation (μm)	572 ± 40	735 ± 92	231 ± 19	666 ± 183*	352 ± 23	320 ± 74	485 ± 46	553 ± 69
Trabecular Number (1/mm)	1.8 ± 0.1	1.4 ± 0.1	4.1 ± 0.3	2.0 ± 0.3*	2.8 ± 0.2	3.3 ± 0.5	2.0 ± 0.2	1.9 ± 0.3
Trabecular Thickness (μm)	11.7 ± 0.6	12.9 ± 0.8	23.5 ± 0.8	20.6 ± 1.2	21.9 ± 0.7	31.5 ± 2.3*	24.4 ± 1.5	24.0 ± 2.0
Osteoblast Surface/Bone Surface (%)	11.8 ± 2.3	11.5 ± 3.0	17.5 ± 1.4	22.4 ± 2.5	16.9 ± 2.3	12.0 ± 2.8	10.5 ± 1.0	14.3± 2.4
Number of Osteoblasts/Bone Perimeter (1/mm)	12.7 ± 2.2	13.5 ± 3.5	15.8 ± 1.2	20.1 ± 2.3	16.3 ± 1.7	11.8 ± 3.1	12.9 ± 1.2	17.0 ± 2.5
Number of Osteoblasts/Tissue Area (1/mm^2)	46 ± 9	36 ± 8	100 ± 9	65 ± 11*	71 ± 10	57 ± 17	40.7 ± 4.0	47.1 ± 4.7
Osteoclast Surface/Bone Surface (%)	12.2 ± 1.2	13.3 ± 0.5	14.0 ± 0.7	14.7 ± 0.9	12.8 ± 0.8	10.6 ± 1.1	15 ± 2	14 ± 2

Males	**10 Day**		**1 Month**		**3 Month**		**6 Month**	
	Wild Type	***Grem1* null**	**Wild Type**	***Grem1* null**	**Wild Type**	***Grem1* null**	**Wild Type**	***Grem1* null**
Number of Osteoclasts/Bone Perimeter (1/mm)	8.8 ± 0.8	9.4 ± 0.4	6.7 ± 0.4	7.3 ± 0.4	6.6 ± 0.5	5.2 ± 0.6	6.9 ± 0.9	6.3 ± 0.7
Number of Osteoclasts/Tissue Area (1/mm^2)	30.2 ± 1.7	26.3 ± 3.0	43 ± 4	22 ± 3*	28 ± 2	26 ± 5	20.9 ± 0.9	18.1 ± 2.4
Eroded Surface/Bone Surface (%)	27.7 ± 2.3	26.7 ± 1.4	26.7 ± 1.5	27.8 ± 1.3	21.3 ± 1.5	16.5 ± 1.6	23 ± 3	21 ± 2
Mineral Apposition Rate (μm/day)			2.01 ± 0.10	1.84 ± 0.11	0.73 ± 0.08	1.12 ± 0.18	0.92 ± 0.52	0.75 ± 0.06
Mineralizing Surface/Bone Surface (%)			5.7 ± 1.0	9.5 ± 1.4*	8.3 ± 0.8	18.6 ± 4.7*	13.8 ± 2.5	11.9 ± 1.5
Bone Formation Rate (μm^3/μm^2/day)			0.113 ± 0.01	0.178 ± 0.031	0.062 ± 0.011	0.162 ± 0.041*	0.128 ± 0.024	0.087 ± 0.009

Bone histomorphometry was performed on femurs from 10 day, 1, 3 and 6 month old male and female *Grem1* null and wild type littermate controls. Values are means ± SEM; n = 4 to 12. Area measured for 10 day old control and experimental mice was 1.27 mm^2 and for 1, 3 and 6 month old mice was 2.59 mm^2.

*Significantly different from controls $p < 0.05$ by unpaired *t* test.

Table 2

Femoral microarchitecture assessed by μCT of 1, 3 and 6 month old male and female *Grem1* null mice and wild type littermate controls.

Males	**1 Month**		**3 Month**		**6 Month**	
	Wild Type	***Grem1* null**	**Wild Type**	***Grem1* null**	**Wild Type**	***Grem1* null**
Bone Volume/Tissue Volume (%)	6.1 ± 0.4	2.9 ± 0.4*	8.4 ± 1.4	8.5 ± 1.6	4.7 ± 0.9	2.7 ± 0.3*
Trabecular Separation (μm)	224 ± 11	343 ± 22*	228 ± 20	221 ± 11	277 ± 12	423 ± 57*
Trabecular Number (1/mm)	4.6 ± 0.2	3.0 ± 0.2*	4.6 ± 0.2	4.5 ± 0.2	3.6 ± 0.1	2.6 ± 0.3*
Trabecular Thickness (μm)	26.9 ± 0.7	25.6 ± 0.5	34.2 ± 1.4	38.8 ± 2.5	35.8 ± 1.4	45.4 ± 3.4*
Connectivity Density (1/mm^3)	211 ± 21	44 ± 11*	226 ± 51	144 ± 37	67 ± 16	2.6 ± 7*
Structure Model Index	2.7 ± 0.05	2.9 ± 0.05*	2.9 ± 0.2	2.5 ± 0.2	2.8 ± 0.2	2.9 ± 0.3
Cortical Thickness (μm)	112 ± 1	97 ± 5*	179 ± 7	186 ± 7	171 ± 4	185 ± 5
Females	1 Month		3 Month		6 Month	
	Wild Type	*Grem1* null	Wild Type	*Grem1* null	Wild Type	*Grem1* null
Bone Volume/Tissue Volume (%)	5.8 ± 0.7	3.6 ± 0.7+	5.0 ± 0.8	5.5 ± 0.9	3.8 ± 0.6	3.5 ± 0.8
Trabecular Separation (μm)	224 ± 16	305 ± 33+	260 ± 12	292 ± 26	351 ± 19	394 ± 15
Trabecular Number (1/mm)	4.6 ± 0.3	3.5 ± 0.4*	3.9 ± 0.2	3.5 ± 0.3	2.9 ± 0.1	2.6 ± 0.1
Trabecular Thickness (μm)	26.3 ± 0.7	26.5 ± 0.9	33.1 ± 1.7	42.2 ± 1.8	39.1 ± 3.5	50.0 ± 5.3
Connectivity Density (1/mm^3)	222 ± 40	78 ± 26*	109 ± 29	66 ± 19	51 ± 8	37 ± 11
Structure Model Index	2.7 ± 0.1	2.9 ± 0.1	2.5 ± 0.2	2.7 ± 0.2	2.9 ± 0.1	3.2 ± 0.3
Cortical Thickness (μm)	119 ± 6	94 ± 6*	177 ± 4	184 ± 9	196 ±3	191 ± 5

Bone μCT was performed on femurs from 1, 3 and 6 month old male and female *Grem1* null and wild type littermate controls. Voxel size used for analysis was 6 μm^3. Values are means ± SEM; n = 5 to 6.

*Significantly different from controls, $p < 0.05$ by unpaired *t* test.

+p <0.057

Table 3

Vertebral microarchitecture assessed by μCT of 1, 3 and 6 month old male and female *Grem1* null mice and wild type littermate controls.

Males	**1 Month**		**3 Month**		**6 Month**	
	Wild Type	***Grem1* null**	**Wild Type**	***Grem1* null**	**Wild Type**	***Grem1* null**
Bone Volume/Tissue Volume (%)	14.9 ± 0.9	11.8 ± 0.6*	24.6 ± 0.7	16.9 ± 1.3*	15.5 ± 1.5	10.1 ± 1.3*
Trabecular Separation (μm)	196 ± 5	209 ± 5	183 ± 4	235 ± 10*	224 ± 15	282 ± 13*
Trabecular Number (1/mm)	5.0 ± 0.1	4.7 ± 0.1	5.6 ± 0.1	4.4 ± 0.2*	4.5 ± 0.3	3.6 ± 0.1*
Trabecular Thickness (μm)	35.1 ± 0.9	32.2 ± 0.2*	45.4 ± 0.9	42.7 ± 0.7*	37.7 ± 1.6	36.4 ± 1.8
Connectivity Density (1/mm^3)	322 ± 23	264 ± 9	221 ± 15	159 ± 12*	188 ± 17	113 ± 20*
Structure Model Index	14.1± 0.1	1.6 ± 0.1	0.4 ± 0.1	0.9 ± 0.1*	0.9 ± 0.1	1.4 ± 0.2*
Females	1 Month		3 Month		6 Month	
	Wild Type	*Grem1* null	Wild Type	*Grem1* null	Wild Type	*Grem1* null
Bone Volume/Tissue Volume (%)	16.6 ± 0.9	12.4 ± 0.9*	20.6 ± 1.6	18.4 ± 2.7	15.1 ± 1.2	11.9 ± 2.0
Trabecular Separation (μm)	185 ± 8	213 ± 11	232 ± 10	256 ± 27	244 ± 8	306 ± 26
Trabecular Number (1/mm)	5.4 ± 0.2	4.7 ± 0.2*	4.6 ± 0.2	4.3 ± 0.4	4.2 ± 0.1	3.5 ± 0.4
Trabecular Thickness (μm)	35.2 ± 1.2	32.7 ± 1.1	45.9 ± 0.2	43.4 ± 2.6	39.2 ± 0.8	36.2 ± 1.7
Connectivity Density (1/mm^3)	389 ± 40	305 ± 25	181.7 ± 13	186.5 ± 35.1	173 ± 20	296 ± 103
Structure Model Index	1.2 ± 0.1	1.5 ± 0.1	0.6 ± 0.1	0.6 ± 0.2	0.7 ± 0.1	0.9 ± 0.2

Bone μCT was performed on vertebrae from 1, 3 and 6 month old male and female *Grem1* null and wild type littermate controls. Voxel size used for analysis was 6 μm^3. Values are means ± SEM; n = 4 to 6.

*Significantly different from controls, $p < 0.05$ by unpaired *t* test.

Table 4

Vertebral histomorphometry of 3 month old male and female *Grem1* null mice and wild type littermate controls.

Males	**Wild Type**	***Grem1* null**
Bone Volume/Tissue Volume (%)	20.7 ± 0.9	10.7 ± 0.3*
Trabecular Separation (μm)	157 ± 5	275 ± 9*
Trabecular Number (1/mm)	5.1 ± 0.1	3.3 ± 0.1*
Trabecular Thickness (μm)	40.6 ± 1.2	32.7 ± 0.6*
Osteoblast Surface/Bone Surface (%)	17.7 ± 1.3	26.2± 2.5*
Number of Osteoblasts/Bone Perimeter (1/mm)	15.5 ± 1.1	23.7 ± 2.3*
Number of Osteoblasts/Tissue Area (1/mm^2)	157 ± 9	153 ± 12
Osteoclast Surface/Bone Surface (%)	6.7 ± 0.6	7.2 ± 0.8
Number of Osteoclasts/Bone Perimeter (1/mm)	3.3 ± 0.3	3.6 ± 0.4
Number of Osteoclasts/Tissue Area (1/mm^2)	33.5 ± 2.8	23.3 ± 2.8*
Eroded Surface/Bone Surface (%)	15.1 ± 1.4	15.5 ± 1.8
Mineral Apposition Rate (μm/day)	1.11 ± 0.06	1.05 ± 0.03
Mineralizing Surface/Bone Surface (%)	2.9 ± 0.3	5.7 ± 0.9*
Bone Formation Rate (μm^3/μm^2/day)	0.033± 0.004	0.061 ± 0.02*
Females	Wild Type	*Grem1* null
Bone Volume/Tissue Volume (%)	15.4 ± 0.5	15.0 ± 3.0
Trabecular Separation (μm)	218 ± 11	246 ± 67
Trabecular Number (1/mm)	3.9 ± 0.2	4.0 ± 0.6
Trabecular Thickness (μm)	39.3 ± 0.9	36.7 ± 2.3
Osteoblast Surface/Bone Surface (%)	26.1 ± 1.5	26.4 ± 4.5
Number of Osteoblasts/Bone Perimeter (1/mm)	22.4 ± 1.4	23.1 ± 4.0
Number of Osteoblasts/Tissue Area (1/mm^2)	176 ± 13	176 ± 35
Osteoclast Surface/Bone Surface (%)	9.6 ± 1.1	8.5 ± 0.7
Number of Osteoclasts/Bone Perimeter (1/mm)	4.7 ± 0.5	4.1 ± 0.4
Number of Osteoclasts/Tissue Area (1/mm^2)	36.5± 3.0	33.6 ± 7.5
Eroded Surface/Bone Surface (%)	21.2 ± 2.6	17.9 ± 1.8

Bone histomorphometry was performed on Lumbar 3 vertebrae from 3 month old male and female *Grem1* null and wild type littermate controls. Values are means ± SEM; n = 4 to 6.

*Significantly different from controls $p < 0.05$ by unpaired *t* test. Dual calcein and demeclocycline labels were present only in 2 control vertebrae from female mice, not allowing proper histomorphometric analysis.